On the Selection of a Tracer for PET Imaging of HER2-Expressing Tumors: Direct Comparison of a ^{124}I-Labeled Affibody Molecule and Trastuzumab in a Murine Xenograft Model

Anna Orlova[1,2], Helena Wållberg[1], Sharon Stone-Elander[3], and Vladimir Tolmachev[1,2,4]

[1]Affibody AB, Bromma, Sweden; [2]Division of Biomedical Radiation Sciences, Department of Oncology, Radiology and Clinical Immunology, Rudbeck Laboratory, Uppsala University, Uppsala, Sweden; [3]Karolinska Pharmacy at Karolinska University Hospital, Solna, and Department of Clinical Neurosciences, Karolinska Institutet, Stockholm, Sweden; and [4]Division of Nuclear Medicine, Department of Medical Sciences, Uppsala University, Uppsala, Sweden

Human epidermal growth factor receptor type 2 (HER2) is a tyrosine kinase, which is often overexpressed in many carcinomas. Imaging HER2 expression in malignant tumors can provide important prognostic and predictive diagnostic information. The use of anti-HER2 tracers labeled with positron-emitting radionuclides may increase the sensitivity of HER2 imaging. The goal of this study was to compare directly 2 approaches for developing anti-HER2 PET tracers: a ^{124}I-labeled monoclonal antibody and a small (7-kDa) scaffold protein, the Affibody molecule. **Methods:** The anti-HER2 Affibody $Z_{HER2:342}$ and humanized monoclonal antibody trastuzumab were labeled with $^{124/125}$I using *p*-iodobenzoate (PIB) as a linker. Cellular processing of both tracers by HER2-expressing cells was investigated. The biodistributions of ^{124}I-PIB-$Z_{HER2:342}$ and ^{125}I-PIB-trastuzumab were compared in BALB/C *nu/nu* mice bearing HER2-expressing NCI-N87 xenografts using paired labels. Small-animal PET of ^{124}I-PIB-$Z_{HER2:342}$ and ^{124}I-PIB-trastuzumab in tumor-bearing mice was performed at 6, 24, and 72 h after injection. **Results:** Both radioiodinated $Z_{HER2:342}$ and trastuzumab bound specifically to HER2-expressing cells in vitro and specifically targeted HER2-expressing xenografts in vivo. Radioiodinated trastuzumab was more rapidly internalized and degraded, which resulted in better retention of radioactivity delivered by $Z_{HER2:342}$. Total uptake of trastuzumab in tumors was higher than that of ^{124}I-PIB-$Z_{HER2:342}$. However, tumor-to-organ ratios were appreciably higher for ^{124}I-PIB-$Z_{HER2:342}$ due to the more rapid clearance of radioactivity from blood and normal organs. The ex vivo results were confirmed by small-animal PET. **Conclusion:** The use of the small scaffold targeting Affibody provides better contrast in HER2 imaging than does the monoclonal antibody.

Received Sep. 11, 2008; revision accepted Dec. 2, 2008.
For correspondence or reprints contact: Anna Orlova, Affibody AB, Box 20137, SE-16102, Bromma, Sweden.
E-mail: anna.orlova@bms.uu.se

Key Words: Affibody molecules; imaging; targeting; xenografts; HER2

J Nucl Med 2009; 50:417–425
DOI: 10.2967/jnumed.108.057919

The development of imaging agents that detect the presence and levels of molecular biomarkers in malignant tumors is a promising direction for nuclear medicine expansion. This new imaging approach, often denoted as molecular imaging, may provide important information for patient stratification for targeted therapies, aid in restaging diseases, and be used to monitor treatment response. Thus, information on the presence of biomarkers in diseased tissue can change patient management.

Members of the human epidermal growth factor receptor (HER) family are important transmembrane tyrosine kinase proteins, whose overexpression is associated with malignant phenotypes. Different approaches for the treatment of tumors that overexpress the HER family proteins are currently available (*1*). One of the members of this receptor family, human epidermal receptor type 2 (HER2; also known as ErbB2), is often overexpressed in breast, ovarian, urinary bladder, prostate, and non–small cell lung cancer and in several other carcinomas (*2*). The expression of HER2 in normal tissues is low or not detectable (*3*). HER2 overexpression results in increased proliferation (*1*) and has both a prognostic and a predictive value for different treatments. Breast cancers expressing HER2 respond well to anthracycline (e.g., doxorubicin)-based chemotherapy (*4*) and treatment based on the humanized monoclonal anti-HER2 antibody trastuzumab (Herceptin; Genentech USA, Inc.) (*5*). The clinical practice guidelines of the American Society of Clinical Oncology and European Group on Tumor

Markers recommend assessment of HER2 expression in all newly diagnosed or recurrent breast carcinomas to select patients who will benefit from treatment with trastuzumab and anthracyclines (*6,7*).

Assessment of HER2 expression by noninvasive imaging could become an important complement to immunohistochemistry or fluorescence in situ hybridization analyses of biopsied tissue, because it could reduce problems with false-negative results. Available evidence suggests that about 20% of current HER2 tests with either immunohistochemistry or fluorescence in situ hybridization are inaccurate (*6,8*). Radionuclide-based molecular imaging may provide information on HER2 expression not only in primary tumors but also in distant metastases not amenable to biopsy. There may be discordance in HER2 status between primary tumors and distant metastases in breast cancers (*9*).

One approach for developing HER2 imaging tracers has been to label therapeutic anti-HER2 monoclonal antibodies (mAbs) with γ- or positron-emitting radioisotopes. For example, ^{111}In-diethylenetriaminepentaacetic acid (DTPA)-trastuzumab has been used to identify breast cancer patients responding to trastuzumab treatment (alone or in combination with chemotherapy) (*10*). However, the detection rate of single tumor lesions using ^{111}In-DTPA-trastuzumab was only 45% (*11*). The sensitivity of antibody-based tracers is limited by the long biodistribution times, slow tumor penetration, and slow blood clearance of the tracers, which reduces target to nontarget contrast.

In vivo molecular detection of HER2 expression might be improved by using smaller enzymatically produced or engineered fragments (*12,13*), positron-emitting labels for intact anti-HER2 mAbs (*14–16*), or a combination of both methods (*17–19*). With appropriately labeled molecules, PET would offer the advantages of better resolution, better registration efficiency, and higher accuracy of in vivo quantification (*20,21*). Preliminary reports from an ongoing clinical trial on the use of ^{89}Zr-trastuzumab for PET have demonstrated promising results (*16*). Because of their faster biodistribution and more rapid blood and whole-body clearance, smaller antibody fragments can potentially improve imaging contrast (*22*). The size of the smallest fragments (single-chain variable fragment [scFv; 27 kDa]) may not be small enough to enable efficient extravasation, good tissue penetration, and fast blood clearance; thus, creating a targeting molecule smaller than an scFv is of interest. Efforts toward finding proteins with improved affinity have been based on different scaffolds (*22*), of which Affibody molecules (Affibody AB) are one example. Affibody molecules are small (6–7 kDa) proteins based on the 58-amino-acid scaffold (Z domain), structurally derived from staphylococcal protein A (*23*). A randomization of 13 surface-exposed amino acids in their 3-helix structure provided a library from which high-affinity binders to different targets have been selected (*24,25*).

Recently, we reported the selection of an anti-HER2 Affibody molecule with an affinity of 22 pM, $Z_{HER2:342}$ (*26*). Using different modifications, we successfully labeled $Z_{HER2:342}$ with ^{111}In, ^{99m}Tc, and radiohalogens for diagnostic and therapeutic applications (*24,25*). Although the majority of published radiolabeled Affibody molecules have been designed as SPECT diagnostics, a few have also been labeled with ^{68}Ga and ^{18}F for PET (*27–29*). The first proof-of-principle study in a limited number of patients, using a microdose of ^{111}In- or ^{68}Ga-1,4,7,10-tetraazacyclododecane-*N,N′,N″,N‴*,-tetraacetic acid (DOTA)-$Z_{HER2:342\text{-}pep2}$, demonstrated the feasibility of visualizing HER2-positive breast cancer (*27*).

We hypothesized that small Affibody-based tracers would provide better imaging sensitivity than would mAbs, even when both were labeled with appropriate positron emitters. A literature analysis (*30*) supported this hypothesis, though the studies were from different laboratories and used different xenograft models, labeling strategies, and experimental techniques. In the present study, the imaging properties of an Affibody molecule and the mAb trastuzumab were directly compared. It was essential to select an appropriate positron-emitting label, because short-lived positron emitters such as ^{68}Ga and ^{18}F are not suitable for mAbs with slow blood clearance. For this reason, we selected ^{124}I (half-life [$t_{1/2}$] = 4.18 d) attached to the $Z_{HER2:342}$ Affibody molecule and to trastuzumab as a *p*-iodobenzoate (PIB). Our previous data (*26,31*) suggest that this linker does not impair the binding of either molecule, whereas direct radioiodination of anti-HER2 Affibody molecules reduces their binding capacity (*32*). Moreover, the indirect radioiodination methods used in this study result in a lower uptake of radioactivity in the thyroid and stomach due to quicker excretion of radiocatabolites (*33*).

Both $Z_{HER2:342}$ and trastuzumab were labeled using ^{124}I-PIB. For some studies, ^{125}I-PIB was used as a full chemical analog of ^{124}I-PIB. Comparative studies of the cellular processing of radioiodinated $Z_{HER2:342}$ and trastuzumab were performed. The biodistributions of ^{124}I-PIB-$Z_{HER2:342}$ and ^{125}I-PIB-trastuzumab were evaluated ex vivo in mice bearing HER2-expressing NCI-N87 xenografts by a paired-label methodology, and the specificity of tumor uptake was confirmed. Imaging of HER2-expressing xenografts with ^{124}I-PIB-$Z_{HER2:342}$ and ^{124}I-PIB-trastuzumab and small-animal PET corroborated our hypothesis and ex vivo results that a faster contrast between target and nontarget tissues could be attained with the HER2-targeting Affibody molecule.

MATERIALS AND METHODS

Materials

The recombinant Affibody molecules $Z_{HER2:342}$ and non-HER2-specific Z_{Taq} were provided by Affibody AB. The mAbs trastuzumab and palivizumab were purchased via Roche AB and Abbott Scandinavia AB, respectively. ^{125}I was purchased from Amersham, and the ^{124}I for this study was kindly provided by IBA Molecular. Chloramine-T and sodium metabisulfite were from Sigma-Aldrich. NAP-5 size-exclusion columns were purchased from Pharmacia and used according to the manufacturer's instruc-

tions. The buffers were prepared from chemicals (analytic grade or better) from Merck. *N*-Succinimidyl-*p*-(trimethylstannyl)benzoate was synthesized in our laboratory according to a protocol described previously (*34*). Radioactivity in biodistribution and in vitro experiments was measured using an automated γ-counter (Wizard 1480; Wallac).

Radioiodination

The $Z_{HER2:342}$ (^{125}I and ^{124}I) and Z_{Taq} (^{125}I) Affibody molecules and trastuzumab (^{125}I and ^{124}I) and palivizumab (^{125}I) were radiolabeled using previously described methods (*26,35*). Briefly, an aqueous solution of 0.1% acetic acid was added to the stock solution of radioiodine to adjust the pH to 5.0. *N*-Succinimidyl-*p*-(trimethylstannyl)benzoate (5 μL, 1 mg/mL in 5% acetic acid in methanol) was added. Iodination was initiated by the addition of chloramine-T (4 mg/mL in water), and the solution was incubated for 5 min at room temperature. Reaction was quenched by adding sodium meta-bisulfite (8 mg/mL in water). The protein (Affibody molecules, 60 μg, 1.5 mg/mL of phosphate-buffered saline [PBS]; mAbs, 300 μg, 3 mg/mL of PBS) was added, and pH was adjusted to 9.0 with borate buffer (0.07 M, pH 9.3). Molar ratios were adjusted to favor attachment of a single prosthetic group per protein molecule. After 1 h of incubation at room temperature, the radiolabeled conjugates were purified on NAP-5 columns eluted with PBS.

Cell Culture

HER2-expressing NCI-N87 cells (gastric adenocarcinoma cells from liver metastases) were purchased from American Type Tissue Culture Collection via LGC Promochem. The cells were cultured in RPMI 1640 medium (Flow) and supplemented with 10% fetal calf serum, 2 mM L-glutamine, 2% penicillin/streptomycin (PEST), and 10 mM *N*-(2-hydroxyethyl)piperazine-*N*′-(2-ethanesulfonic acid) buffer (all from Biokrom) and 1 mM sodium pyruvate (Sigma-Aldrich) in a humidified incubator (37°C, 5% CO_2).

In Vitro Experiments

In Vitro Cell-Binding Specificity Assay. All radioiodinated conjugates were tested for specific binding to HER2 receptors using the NCI-N87 cells. Briefly, radiolabeled conjugates were added to the cultured cells (Petri dishes: diameter, 2 cm, 5×10^5 cells per dish, 3 dishes per data point) in a concentration of 0.75 pmol/mL. One set of dishes for each conjugate was treated in advance (5 min before adding labeled tracers) with the corresponding nonlabeled protein (100-fold molar excess over labeled tracer) to saturate HER2 receptors on the cells. One set of dishes for ^{125}I-PIB-$Z_{HER2:342}$ was treated in advance with nonlabeled trastuzumab in blocking concentrations, and 1 set for ^{125}I-PIB-trastuzumab was pretreated with nonlabeled $Z_{HER2:342}$. The cells were incubated for 1 h at 37°C, and the incubation medium was collected. Cells were detached using 0.5 mL of a trypsin-ethylenediaminetetraacetic acid solution; after resuspension with an additional 0.5 mL of medium, the cell suspension was collected. Radioactivity in the samples was measured, and cell-associated radioactivity was calculated.

Cellular Processing

The cellular processing of ^{125}I-PIB-$Z_{HER2:342}$ and ^{125}I-PIB-trastuzumab was studied in NCI-N87 cells. The radiolabeled conjugates were added to cultured cells (Petri dishes: diameter, 3.5 cm, 5×10^5 cells per dish, 3 dishes per data point) in a concentration of 37.5 pmol/mL, and the cells were incubated on ice for 2 h to prevent internalization. The incubation medium was changed, and the cells were further incubated at 37°C. At predetermined times (0–24 h), the incubation medium from 1 set of dishes was collected, and the cells were treated with urea (0.5 mL, 4 M solution in 0.2 M glycine buffer, pH 2.0) for 5 min at 4°C to remove the membrane-bound proteins (*36*). The acid solution was collected, and the cells were washed with an additional 0.5 mL of buffer. The combined sample (1 mL) represented the membrane-bound protein. The remaining cell-associated radioactivity (considered as internalized) was removed by treating the cells with sodium hydroxide (1 M, 0.5 mL) for 30 min at 37°C and then washing with the same volume of sodium hydroxide. The radioactivity in the samples was measured, and the cell-associated, membrane-bound, and internalized radioactivities were calculated.

Amounts of Radiocatabolites in the Incubation Medium

For determining the radiocatabolites released from the cells, the incubation medium collected during the cellular-processing experiment was separated on size-exclusion NAP-5 columns (saturated in advance with 2.5% bovine albumin) into high- and low-molecular-weight fractions, which were measured for radioactivity content.

Biodistribution in Tumor-Bearing Mice

Animal experiments were approved by the local Ethics Committee for Animal Research. NCI-N87 xenografts were established in female BALB/c *nu/nu* mice (10–12 wk old on arrival) 4 wk before the experiments by implanting subcutaneously approximately 2×10^6 cells on the right hind leg. The mice were randomly divided into groups of 4.

Three groups were injected intravenously (tail vein) with a PBS solution (100 μL) of ^{124}I-PIB-$Z_{HER2:342}$ and ^{125}I-PIB-trastuzumab (5 μg of Affibody molecule, 20 kBq, plus 30 μg of mAb, 20 kBq). The mice were sacrificed at 6, 24, and 72 h after injection; the organs were dissected and weighed, and their radioactivity content was measured. The whole spectrum was recorded for each sample. ^{125}I counts were measured in a window of 30–80 keV, and ^{124}I counts were measured in a window from 400 to 1,200 keV. The data were corrected for background, dead time, and spillover. The tissue uptake was calculated as the percentage of injected radioactivity per gram of tissue (%IA/g).

To demonstrate that the tumor uptake was receptor-mediated, we performed 2 specificity tests. In a receptor saturation test, 1 group of animals was injected subcutaneously with 4 mg of nonlabeled trastuzumab 14 h before the radioactive injections, and another group was injected with 0.6 mg of nonlabeled Affibody molecules 1 h before the radioactive injections. Both groups were intravenously injected with ^{124}I-PIB-$Z_{HER2:342}$ and ^{125}I-PIB-trastuzumab as described above. These animals were sacrificed at 24 h after injection.

The tumor uptake of nonspecific proteins was evaluated using an anti-Taq polymerase Z_{Taq} Affibody molecule and the antiviral humanized palivizumab. Both were labeled with ^{125}I-PIB in the same way as the ^{124}I-PIB-$Z_{HER2:342}$ and ^{125}I-PIB-trastuzumab. One group of mice was intravenously injected with ^{125}I-PIB-Z_{Taq} (4 μg, 30 kBq) in 100 μL of PBS and another with ^{125}I-PIB-palivizumab (20 μg, 30 kBq) in 100 μL of PBS. Mice were sacrificed at 6 h after injection for ^{125}I-PIB-Z_{Taq} and at 24 h after injection for ^{125}I-PIB-palivizumab.

PET

NCI-N87 xenografts were established for about 4 wk, as described above. The tumors had an average diameter of about

0.5 cm^3 on the day of the experiment. Animals were randomly divided into 6 groups of 3 mice. Three groups were intravenously injected with ^{124}I-PIB-$Z_{HER2:342}$ (1.2 MBq, 5 μg of Affibody molecule in 100 μL of PBS), and another 3 groups were injected with ^{124}I-PIB-trastuzumab (0.8 MBq, 30 μg of mAb in 100 μL of PBS). The mice were euthanized with a lethal intraperitoneal dose of ketamine (Ketalar; Pfizer) and xylazine (Rompun; Mobay Corp.) at 6, 24, and 72 h after injection. The urinary bladders were dissected, and the mice were put on ice until imaging was performed using a microPET Focus120 (CTI Concorde Microsystems). Data were processed with microPET manager (CTI Concorde Microsystems) and evaluated using ASIPro (CTI Concorde Microsystems) and Inveon Research Workplace (Siemens) software. Data were acquired (30–45 min) in fully 3-dimensional mode, and images were reconstructed by a 2-dimensional ordered-subsets expectation maximization algorithm. The matrix size of the reconstructed images was 128 × 128 × 95, with a spatial resolution of 1.3 mm. The data were normalized and corrected for randoms, dead time, and decay.

RESULTS

Radioiodination

All compounds were successfully radioiodinated. Overall yields after size-exclusion purification were 57% for ^{125}I-PIB-$Z_{HER2:342}$, 17.5% for ^{124}I-PIB-$Z_{HER2:342}$, 34% for ^{125}I-PIB-Z_{Taq}, 57% for ^{125}I-PIB-trastuzumab, 18% for ^{124}I-PIB-trastuzumab, and 12% for ^{125}I-PIB-palivizumab.

In Vitro Binding Specificity Assay

The binding of ^{125}I-PIB-Z_{Taq} and ^{125}I-PIB-palivizumab (both of which have no affinity toward HER2) to NCI-N87 cells was negligible and showed no sign of saturation. Radioiodinated $Z_{HER2:342}$ and trastuzumab both bound to HER2-expressing cells specifically (Fig. 1), because binding could be prevented by saturation of the receptors in advance with blocking amounts of the nonlabeled counterpart protein. The Affibody molecule and mAb did not reduce each other's binding in cross-blocking experiments, indicating that they bind to different epitopes of HER2.

Cellular Processing

NCI-N87 cells were incubated on ice with ^{125}I-PIB-$Z_{HER2:342}$ and ^{125}I-PIB-trastuzumab; after the incubation medium was changed, their cellular processing was studied (Fig. 2). For both tracers, the cell-associated radioactivity decreased with time but in a different manner (Figs. 2A and 2B). For ^{125}I-PIB-trastuzumab, the cell-associated radioactivity decreased constantly, and after 24 h more than 50% radioactivity had been lost from the cells. For ^{125}I-PIB-$Z_{HER2:342}$, about 30% of the radioactivity was lost within the first 30 min, followed thereafter by a slow decrease. This second phase of radioactivity release for ^{125}I-PIB-$Z_{HER2:342}$ was much slower than for the trastuzumab conjugate, and the final cell-associated radioactivity for the Affibody conjugate at 24 h was higher than for the antibody (53% ± 1% and 45.8% ± 0.3% of initial radioactivity, respectively).

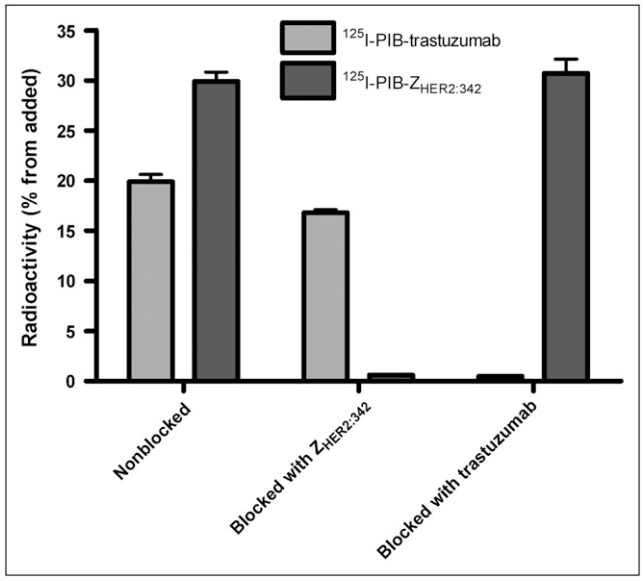

FIGURE 1. In vitro specificity test for ^{125}I-PIB-$Z_{HER2:342}$ and for ^{125}I-PIB-trastuzumab on NCI-N87 cells. Radiolabeled conjugates were added to culture cells at a 1:1 ratio of conjugated molecule to HER2 receptor. For both conjugates, cells in control dishes were treated with nonlabeled Affibody molecule or trastuzumab with 100-fold excess over receptors. Data are presented as average value from 3 Petri dishes ± SD. Error bars might not be seen because they are smaller than point symbols.

The internalized radioactivity was low (<12%) at all time points for both tracers. The release of low-molecular-weight radioactivity into the incubation medium was greater for trastuzumab: 70% of the radioactivity in the medium after 24 h was fragments (radiocatabolites), with molecular weights lower than 5 kDa (Figs. 2C and 2D). The release of low-molecular-weight radiocatabolites for the Affibody was much slower, less than 40% after 24 h.

Biodistribution of ^{124}I-PIB-$Z_{HER2:342}$ and ^{125}I-PIB-Trastuzumab

Tumor targeting and biodistribution of ^{124}I-PIB-$Z_{HER2:342}$ and ^{125}I-PIB-trastuzumab were studied at 6, 24, and 72 h after injection in BALB/c *nu/nu* mice bearing HER2-expressing NCI-N87 xenografts in dual-isotope experiments. The results are shown in Table 1, and the calculated tumor-to-nontumor ratios are presented in Table 2.

The biodistribution of ^{124}I-PIB-$Z_{HER2:342}$ at 6 and 24 h after injection was similar to previously published data for ^{125}I-PIB-$Z_{HER2:342}$ in other xenograft models (*26*). The clearance of radioiodinated PIB-$Z_{HER2:342}$ from blood and healthy tissues was rapid, and the concentration of radioactivity in NCI-N87 xenografts exceeded that in all studied organs as early as 6 h after injection. The levels of uptake of ^{124}I-PIB-$Z_{HER2:342}$ in NCI-N87 xenografts were lower than that previously observed in SKOV-3 xenografts (*26*), which could reflect either a lower level of HER2 expression or a lower vascular permeability in the NCI-N87 xenografts

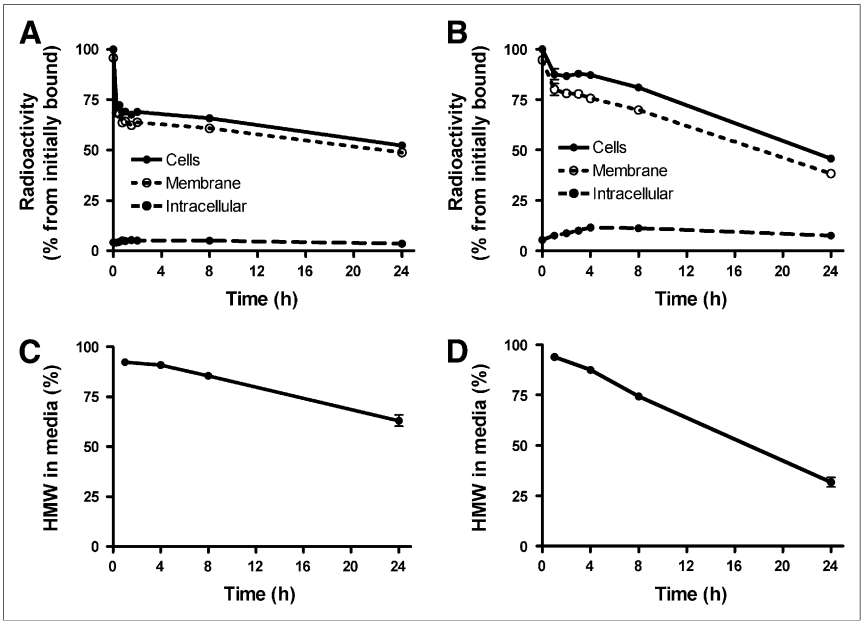

FIGURE 2. Cellular retention of radioactivity after interrupted incubation of HER2-expressing NCI-N87 cells with HER2-targeting Affibody molecules ^{125}I-PIB-$Z_{HER2:342}$ (A) and ^{125}I-PIB-trastuzumab (B). (C) Radioactivity associated with high-molecular-weight fraction in incubation medium for ^{125}I-PIB-$Z_{HER2:342}$. (D) Radioactivity associated with high-molecular-weight fraction in incubation medium for ^{125}I-PIB-trastuzumab. Data are presented as average value from 3 Petri dishes ± SD. Error bars might not be seen because they are smaller than point symbols.

model. The radioactivity concentrations in the xenografts decreased with time but much more slowly than the clearance from healthy tissue. Therefore, the tumor-to-blood ratios increased over time and were 8 ± 2, 16 ± 5, and 27 ± 17 at 6, 24, and 72 h after injection, respectively.

The clearance of ^{125}I-PIB-trastuzumab from blood and healthy tissues was much slower than that of ^{124}I-PIB-$Z_{HER2:342}$. The tumor uptake of the mAb was stable, but the slow kinetics led to low tumor-to-blood ratios, even on day 3 after injection (1.3 ± 0.4). This resulted in appreciably higher tumor-to-organ ratios for ^{124}I-PIB-$Z_{HER2:342}$ than for ^{125}I-PIB-trastuzumab. For both radioiodinated conjugates, no accumulation of radioactivity was found in the salivary gland, stomach, and thyroid, indicating that no release of free iodide occurred and catabolites were rapidly excreted via urine.

In Vivo Specificity

The results of the in vivo saturation of HER2 receptors with nonlabeled $Z_{HER2:342}$ or trastuzumab demonstrate that the tumor accumulation of both conjugates was receptor-specific (Table 3), because an injection in advance of a large excess of protein reduced the tumor uptake of ^{124}I-PIB-$Z_{HER2:342}$ from 1.4% ± 0.3%IA/g to 0.8% ± 0.1%IA/g ($P < 0.001$) and of ^{125}I-PIB-trastuzumab from 16% ± 3%IA/g to 5.3% ± 0.3%IA/g ($P < 0.0005$). In agreement with in vitro data, the Affibody molecule did not block trastuzumab binding nor did trastuzumab block the binding of Affibody molecule to HER2 receptors. The tumor accumulation of the non-HER2-specific Affibody molecule (^{125}I-PIB-$Z_{Taq:}$) or antibody (^{125}I-PIB-palivizumab) was approximately 10-fold lower than that of their specific counterparts in NCI-N87 xenografts ($P < 0.005$ for both tracers). In both cases, the tumor concentration of radioactivity was lower than the blood concentration.

PET of HER2 Expression in NCI-N87 Xenografts

Figure 3 shows representative PET images for ^{124}I-PIB-$Z_{HER2:342}$ and ^{124}I-PIB-trastuzumab in NCI-N87 xenograft–bearing BALB/c *nu/nu* mice. In agreement with ex vivo measurements, the radioactivity concentrations in tumors in mice injected with the Affibody molecule exceeded those in all other organs at 6 h after injection. At 24 h after injection, the tumor uptake completely dominated the image. In mice injected with ^{124}I-PIB-trastuzumab, the tumors were visualized at 6 h after injection, but high radioactivity concentration in the blood led to visualization of the heart, main blood vessels, and well-perfused organs (e.g., liver). Target to nontarget contrast with ^{124}I-PIB-trastuzumab improved with time but even at 72 h after injection did not reach the quality achieved with ^{124}I-PIB-$Z_{HER2:342}$ at 6 h after injection.

DISCUSSION

The results of this study demonstrated that both ^{124}I-PIB-trastuzumab and ^{124}I-PIB-$Z_{HER2:342}$ are capable of specifically targeting HER2-expressing xenografts and clearly revealing them in PET scans. However, tumor-to-nontumor ratios with ^{124}I-PIB-$Z_{HER2:342}$ were much higher, yielding better contrast and imaging sensitivity, particularly in organs that are frequently sites for metastases. These data suggest that this Affibody molecule can be a better tracer than trastuzumab for PET of HER2 expression in primary cancer and in distant metastases.

The use of radiolabeled trastuzumab is a straightforward and practical approach for detecting HER2-expressing tumors. The antibody is commercially available, and clinical trials have demonstrated its safety. Using PET can further improve the imaging sensitivity in clinics (*16*). The results of the present study also confirmed that radiolabeled

TABLE 1. Biodistribution of ^{124}I-PIB-$Z_{HER2:342}$ and ^{125}I-PIB-Trastuzumab After Injection in BALB/C *nu/nu* Mice Bearing HER2-Expressing NCI-N87 Xenografts

Location	Biodistribution		
	6 h	24 h	72 h
^{124}I-PIB-$Z_{HER2:342}$			
Blood	0.59 ± 0.05	0.09 ± 0.02	0.021 ± 0.008
Lung	0.8 ± 0.2	0.5 ± 0.1	0.2 ± 0.1
Liver	0.84 ± 0.09	0.20 ± 0.07	0.077 ± 0.008
Spleen	0.9 ± 0.2	0.4 ± 0.2	0.18 ± 0.05
Stomach	1 ± 1	0.32 ± 0.09	0.14 ± 0.07
Kidney	3.2 ± 0.4	0.19 ± 0.01	0.11 ± 0.02
Salivary gland	0.8 ± 0.3	NM	NM
Thyroid*	0.2 ± 0.2	NM	NM
Tumor	4.7 ± 1.0	1.4 ± 0.3	0.4 ± 0.1
Muscle	0.10 ± 0.05	NM	NM
Intestines with content*	1.3 ± 0.22	0.07 ± 0.01	0.05 ± 0.02
Carcass*	2.4 ± 0.1	0.7 ± 0.1	0.17 ± 0.02
^{125}I-PIB-trastuzumab			
Blood	18 ± 3	13 ± 2	9 ± 2
Lung	6.5 ± 1.0	5. 6 ± 0.9	3.3 ± 0.6
Liver	4.7 ± 0.3	3.1 ± 0.6	1.9 ± 0.6
Spleen	6 ± 1	5 ± 2	1.8 ± 0.6
Stomach	1.5 ± 0.6	1.3 ± 0.4	0.8 ± 0.3
Kidney	6.5 ± 1.0	5.1 ± 0.3	3.0 ± 0.5
Salivary gland	2.3 ± 0.4	2.8 ± 0.5	1.7 ± 0.5
Thyroid*	0.08 ± 0.02	0.16 ± 0.06	0.041 ± 0.006
Tumor	14 ± 7	16 ± 3	12 ± 3
Muscle	0.7 ± 0.1	1.3 ± 0.1	0.62 ± 0.08
Intestines with content*	4.0 ± 0.6	2.7 ± 0.2	1.7 ± 0.4
Carcass*	20 ± 3	21.0 ± 0.7	15 ± 4

*Data for thyroid, intestines with content, and carcass are given as %IA per whole sample.
NM = nonmeasurable (counts per sample were less than 2 times background counts).
Data are presented as an average %IA/g and SD (n = 4).

trastuzumab is a good tracer: the HER2-expressing xenografts were visualized as early as 6 h after injection. The specificity of the visualization was confirmed in this study by 2 independent methods. The problem, however, was the slow clearance from blood of the tracer. The small-animal PET images showed that imaging metastases in the liver would be complicated until 72 h after injection due to the high level of blood-borne radioactivity in this well-perfused organ. This high level of radioactivity is a serious limitation for the use of radiolabeled trastuzumab because the liver is a common metastatic site for breast cancer, the main target for anti-HER2 therapy.

^{124}I-PIB-$Z_{HER2:342}$ provided better imaging contrast (tumor-to-organ ratios) at 6 h after injection than did ^{124}I-PIB-trastuzumab at 72 h after injection. Being able to image on the day of the administration offers apparent clinical, logistic, and economic advantages for routine use of a tracer. The ex vivo tumor-to-organ ratios (Table 2) provided a quantitative confirmation of the small-animal PET findings. The contrast enhancement for ^{124}I-PIB-$Z_{HER2:342}$ was due to the much more rapid clearance from blood and nonspecific compartments (Table 1). The absolute tumor accumulation of ^{124}I-PIB-$Z_{HER2:342}$ was lower than that of ^{124}I-PIB-trastuzumab, also because of the rapid clearance. However, the uptake level 6 h after injection (4.7% ± 1.0%IA/g) was similar to that of ^{111}In-pentetreotide (OctreoScan; Covidien) in a murine model (3.03 ± 0.26%IA/g) (*37*). The successful clinical use of ^{111}In-pentetreotide suggests that this level of accumulation can be adequate for routine diagnostics.

We studied in detail the cellular processing of both radioiodinated conjugates (^{125}I-PIB-$Z_{HER2:342}$ and ^{125}I-PIB-trastuzumab) by the HER2-expressing cell line NCI-N87. We found 2 different processing modes for the tested conjugates, which can influence their in vivo behavior and tumor targeting. Labeled trastuzumab was readily internalized, and after rapid degradation low-molecular-weight (<5 kDa) radiocatabolites were excreted (eliminated) in the medium. The radioiodinated Affibody molecule, however, remained firmly bound to the cell surface and escaped rapid degradation, resulting in a better overall retention of ^{125}I-PIB-$Z_{HER2:342}$. These data are in agreement with published data for these proteins obtained on other cell lines and using other labeling methods (*36,38*). These results raise the question of whether an adequate label was selected for the trastuzumab—for example, whether a residualizing label such as ^{89}Zr would not have been superior. Indeed, the use of the ^{89}Zr label instead of ^{124}I

TABLE 2. Tumor-to-Nontumor Ratio in BALB/c *nu/nu* Mice Bearing HER2-Expressing NCI-N87 Xenografts After Intravenous Injection of ^{124}I-PIB-$Z_{HER2:342}$ and ^{125}I-PIB-Trastuzumab

Location	Ratio		
	6 h	24 h	72 h
^{124}I-PIB-$Z_{HER2:342}$			
Blood	8 ± 2	16 ± 5	27 ± 17
Lung	6 ± 2	2.9 ± 1.0	5 ± 5
Liver	5.6 ± 0.6	8 ± 3	6 ± 2
Spleen	5.6 ± 0.8	4 ± 2	3 ± 1
Stomach	5 ± 3	4.5 ± 1.0	5 ± 5
Kidney	1.5 ± 0.3	8 ± 1	4 ± 1
Salivary gland	7 ± 2	NM	NM
Muscle	53 ± 14	NM	NM
^{125}I-PIB-trastuzumab			
Blood	0.8 ± 0.4	1.2 ± 0.3	1.3 ± 0.4
Lung	2 ± 1	2.8 ± 0.2	4 ± 1
Liver	3 ± 1	5.1 ± 0.9	7 ± 2
Spleen	2 ± 1	4 ± 1	7 ± 1
Stomach	9 ± 2	13 ± 3	14 ± 2
Kidney	2.1 ± 0.8	3.1 ± 0.5	3.9 ± 0.4
Salivary gland	6 ± 3	5.6 ± 0.5	6.9 ± 0.7
Muscle	21 ± 9	12 ± 2	19 ± 3

Data are presented as average of 4 animals and SD. Radioactivity contents in salivary glands and muscle at 24 and 72 h after injection of ^{124}I-PIB-$Z_{HER2:342}$ were nonmeasurable (NM) (counts per sample were less than 2 times background counts).

for U36 mAb increased the tumor uptake 1.45-fold at 72 h after injection (*39*). However, the liver uptake was also increased 4-fold for ^{89}Zr-U36. Thus, the contrast toward this important metastatic site would not be improved. In the case of $Z_{HER2:342}$, the use of a nonresidualizing iodine label might be an advantage. Because of slow internalization, the nonresidualizing nature of iodine, compared with the residualizing radiometal labels, has little influence on the tumor retention but does facilitate radioactivity clearance from the kidneys (*26,40,41*).

Another important finding is that $Z_{HER2:342}$ and trastuzumab bind to different epitopes of HER2, as was confirmed in this study both in vitro (Fig. 1) and ex vivo (Table 3). Taking advantage of this difference may provide a unique opportunity for monitoring HER2 expression levels during trastuzumab therapy or combination therapies including trastuzumab by using $Z_{HER2:342}$ as the imaging biomarker. Using a radiolabeled trastuzumab for the same kind of studies would always entail an uncertainty as to whether a reduced tumor uptake would be due to downregulation of the receptor or to receptor saturation by the nonlabeled mAb.

In addition to the use of the ^{124}I-PIB linker, 3 other approaches for labeling Affibody molecules for PET applications have been reported recently. A synthetic DOTA-$Z_{HER2:342\text{-}pep2}$ has been labeled with ^{68}Ga ($t_{1/2}$ = 67.6 min) (*27*). Cysteine-containing Affibody molecules have been site-specifically labeled with ^{18}F ($t_{1/2}$ = 109.8 min) using *N*-2-(4-^{18}F-fluorobenzamido)ethyl]maleimide (*28*) and ^{18}F-*N*-(4-fluorobenzylidene)oxime (*29*). This diversity creates opportunities for selecting the most suitable Affibody-based anti-HER2 tracer for each clinical site. The straightforward labeling chemistry of ^{68}Ga could enable reproducible tracer preparations, even in PET centers without their own cyclotron. This approach might be promising when ^{68}Ge/^{68}Ga generators approved for routine clinical use are readily available. ^{18}F-fluoride is already readily available at many PET centers because of the widespread production of ^{18}F-FDG. Radiofluorinated Affibody molecules could similarly be distributed to regional satellite PET centers. The long half-life of ^{124}I would enable a worldwide distribution of ^{124}I-PIB-$Z_{HER2:342}$ from a centralized production facility. An advantage of this approach is that the labeling would be performed by a well-trained and experienced staff, potentially reducing the logistics issue involved in making this radiodiagnostic more quickly available as a routine imaging diagnostic.

CONCLUSION

Affibody molecules for the imaging of HER2 expression in tumors provide better contrast (tumor-to-organ ratios) and at an earlier time than is achieved with radiolabeled trastuzumab. The radiolabeled Affibody may also provide a

TABLE 3. In Vivo HER2-Targeting Specificity for ^{124}I-PIB-$Z_{HER2:342}$ and ^{125}I-PIB-Trastuzumab

		^{124}I-PIB-$Z_{HER2:342}$				^{125}I-PIB-trastuzumab			
Time (h)	Location	Nonblocked	Blocked with $Z_{HER2:342}$	Blocked with trastuzumab	^{125}I-PIB-$Z_{Taq:}$	Nonblocked	Blocked with $Z_{HER2:342}$	Blocked with trastuzumab	^{125}I-PIB-palivizumab
6	Blood	0.59 ± 0.05			0.5 ± 0.1				
	Tumor	4.7 ± 1.0			0.3 ± 0.2				
24	Blood	0.09 ± 0.02	0.19 ± 0.01	0.16 ± 0.02		13 ± 2	14 ± 1	13 ± 2	7.0 ± 0.5
	Tumor	1.4 ± 0.3	0.8 ± 0.1	1.9 ± 0.4		16 ± 3	19 ± 2	5.3 ± 0.3	1.9 ± 0.1

Tumor targeting of radioiodinated Affibody molecule and trastuzumab was compared in BALB/c *nu/nu* mice with NCI-N87 xenografts with that for mice injected in advance with blocking amounts of nonlabeled Affibody molecule (1 h before injection of ^{124}I-PIB-$Z_{HER2:342}$/^{125}I-PIB-trastuzumab) or trastuzumab (24 h before injection of ^{124}I-PIB-$Z_{HER2:342}$/^{125}I-PIB-trastuzumab) and unspecific to HER2 Affibody molecule ^{125}I-PIB-Z_{Taq} and ^{125}I-PIB-palivizumab.

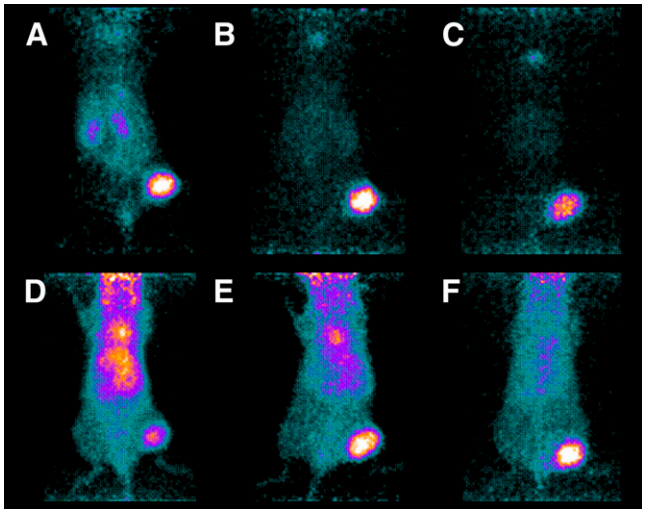

FIGURE 3. Small-animal PET images of uptake in NCI-N87 xenografts relative to other tissues of ^{124}I-PIB-$Z_{HER2:342}$ (A–C) and ^{124}I-PIB-trastuzumab (D–F) in representative mice sacrificed at 6 (A and D), 24 (B and E), and 72 h (C and F) after intravenous injection of Affibody molecule (1.2 MBq) or of mAb (0.8 MBq). Urinary bladders were dissected before scanning for 30–45 min.

superior imaging tool with which fluctuations in HER2 levels can be monitored throughout therapeutic protocols that include trastuzumab.

ACKNOWLEDGMENTS

We thank the animal facility staff of Rudbeck laboratory and Li Lu of the KI MicroPET imaging facility for technical assistance. We thank Dr. Monica Hansson, Dr. Anders Wennborg, and Dr. Lars Abrahmsén (Affibody AB) for interesting and inspiring discussions on the use of Affibody molecules for imaging and for comments on the manuscript. ^{124}I was kindly provided for this study by IBA Molecular. This study was financially supported by a grant from the Swedish Cancer Society (Cancerfonden), and the microPET scanner was purchased through a grant from the Swedish Research Council (Vetenskapsrådet, 2004-5104).

REFERENCES

1. Marmor MD, Skaria KB, Yarden Y. Signal transduction and oncogenesis by ErbB/HER receptors. *Int J Radiat Oncol Biol Phys.* 2004;58:903–913.
2. Carlsson J. EGFR-family expression and implications for targeted radionuclide therapy. In: Stigbrand T, Carlsson J, Adams G, eds. *Targeted Radionuclide Tumor Therapy: Biological Aspects.* Dordrecht, The Netherlands: Springer; 2008:25–58.
3. Human Protein Atlas. Available at: http://www.proteinatlas.org/. Accessed January 2, 2009.
4. Muss HB, Thor AD, Berry DA, et al. c-erbB-2 expression and response to adjuvant therapy in women with node-positive early breast cancer. *N Engl J Med.* 1994;330:1260–1266.
5. Slamon DJ, Leyland-Jones B, Shak S, et al. Use of chemotherapy plus a monoclonal antibody against HER2 for metastatic breast cancer that overexpresses HER2. *N Engl J Med.* 2001;344:783–792.
6. Wolff AC, Hammond ME, Schwartz JN, et al. American Society of Clinical Oncology/College of American Pathologists guideline recommendations for human epidermal growth factor receptor 2 testing in breast cancer. *J Clin Oncol.* 2007;25:118–145.
7. Molina R, Barak V, van Dalen A, et al. Tumor markers in breast cancer: European Group on Tumor Markers recommendations. *Tumour Biol.* 2005;26:281–293.
8. Bartlett J, Mallon E, Cooke T. The clinical evaluation of HER-2 status: which test to use? *J Pathol.* 2003;199:411–417.
9. Zidan J, Dashkovsky I, Stayerman C, et al. Comparison of HER-2 overexpression in primary breast cancer and metastatic sites and its effect on biological targeting therapy of metastatic disease. *Br J Cancer.* 2005;93:552–556.
10. Behr TM, Behe M, Wormann B. Trastuzumab and breast cancer. *N Engl J Med.* 2001;345:995–996.
11. Perik PJ, Lub-De Hooge MN, Gietema JA, et al. Indium-111-labeled trastuzumab scintigraphy in patients with human epidermal growth factor receptor 2-positive metastatic breast cancer. *J Clin Oncol.* 2006;24:2276–2282.
12. Olafsen T, Tan GJ, Cheung CW, et al. Characterization of engineered anti-p185HER-2 (scFv-CH3)2 antibody fragments (minibodies) for tumor targeting. *Protein Eng Des Sel.* 2004;17:315–323.
13. Tang Y, Wang J, Scollard DA, et al. Imaging of HER2/neu-positive BT-474 human breast cancer xenografts in athymic mice using ^{111}In-trastuzumab (Herceptin) Fab fragments. *Nucl Med Biol.* 2005;32:51–58.
14. Garmestani K, Milenic DE, Plascjak PS, Brechbiel MW. A new and convenient method for purification of ^{86}Y using a Sr(II) selective resin and comparison of biodistribution of ^{86}Y and ^{111}In labeled Herceptin. *Nucl Med Biol.* 2002;29:599–606.
15. Bruskin A, Sivaev I, Persson M, et al. Radiobromination of monoclonal antibody using potassium [^{76}Br](4 isothiocyanatobenzyl-ammonio)-bromo-decahydro-closo-dodecaborate (Bromo-DABI). *Nucl Med Biol.* 2004;31:205–211.
16. Dijkers E, Lub-de Hooge MN, Kosterink JG, et al. Characterization of ^{89}Zr-trastuzumab for clinical HER2 immunoPET imaging [abstract]. *J Clin Oncol.* 2007;25(suppl 18):S3508.
17. Smith-Jones PM, Solit DB, Akhurst T, Afroze F, Rosen N, Larson SM. Imaging the pharmacodynamics of HER2 degradation in response to Hsp90 inhibitors. *Nat Biotechnol.* 2004;22:701–706.
18. Olafsen T, Kenanova VE, Sundaresan G, et al. Optimizing radiolabeled engineered anti-p185HER2 antibody fragments for in vivo imaging. *Cancer Res.* 2005;65:5907–5916.
19. Robinson MK, Doss M, Shaller C, et al. Quantitative immuno-positron emission tomography imaging of HER2-positive tumor xenografts with an iodine-124 labeled anti-HER2 diabody. *Cancer Res.* 2005;65:1471–1478.
20. Lundqvist H, Lubberink M, Tolmachev V, et al. Positron emission tomography and radioimmunotargeting: general aspects. *Acta Oncol.* 1999;38:335–341.
21. Verel I, Visser GW, van Dongen GA. The promise of immuno-PET in radioimmunotherapy. *J Nucl Med.* 2005;46(suppl 1):164S–171S.
22. Van de Wiele C, Revets H, Mertens N. Radioimmunoimaging: advances and prospects. *Q J Nucl Med Mol Imaging.* 2004;48:317–325.
23. Nygren PA. Alternative binding proteins: affibody binding proteins developed from a small three-helix bundle scaffold. *FEBS J.* 2008;275:2668–2676.
24. Tolmachev V, Orlova A, Nilsson FY, Feldwisch J, Wennborg A, Abrahmsén L. Affibody molecules: potential for in vivo imaging of molecular targets for cancer therapy. *Expert Opin Biol Ther.* 2007;7:555–568.
25. Orlova A, Feldwisch J, Abrahmsén L, Tolmachev V. Update: affibody molecules for molecular imaging and therapy for cancer. *Cancer Biother Radiopharm.* 2007;22:573–584.
26. Orlova A, Magnusson M, Eriksson T, et al. Tumor imaging using a picomolar affinity HER2 binding Affibody molecule. *Cancer Res.* 2006;66:4339–4348.
27. Baum RP, Orlova A, Tolmachev V, Feldwisch J. A novel molecular imaging agent for diagnosis of recurrent HER2 positive breast cancer: first time in human study using an indium-111- or gallium-68-labeled Affibody molecule [abstract]. *Eur J Nucl Med Mol Imaging.* 2006;33(suppl):S91.
28. Kramer-Marek G, Kiesewetter DO, Martiniova L, Jagoda E, Lee SB, Capala J. [^{18}F]FBEM-$Z_{HER2:342}$-Affibody molecule: a new molecular tracer for in vivo monitoring of HER2 expression by positron emission tomography. *Eur J Nucl Med Mol Imaging.* 2008;35:1008–1018.
29. Cheng Z, De Jesus OP, Namavari M, et al. Small-animal PET imaging of human epidermal growth factor receptor type 2 expression with site-specific ^{18}F-labeled protein scaffold molecules. *J Nucl Med.* 2008;49:804–813.
30. Tolmachev V. Imaging of HER-2 overexpression in tumors for guiding therapy. *Curr Pharm Des.* 2008;14:2999–3019.
31. Persson M, Sivaev I, Winberg KJ, Gedda L, Malmström PU, Tolmachev V. In vitro evaluation of two polyhedral boron anion derivatives as linkers for attachment of radioiodine to anti-HER2 monoclonal antibody trastuzumab. *Cancer Biother Radiopharm.* 2007;22:585–596.
32. Steffen AC, Wikman M, Tolmachev V, et al. In vitro characterization of a bivalent anti-HER-2 affibody with potential for radionuclide-based diagnostics. *Cancer Biother Radiopharm.* 2005;20:239–248.

33. Tolmachev V, Orlova A, Lundqvist H. Approaches to improve cellular retention of radiohalogen labels delivered by internalising tumor-targeting proteins and peptides. *Curr Med Chem.* 2003;10:2447–2460.
34. Koziorowski J, Henssen C, Weinreich R. A new convenient route to radioiodinated *N*-succinimidyl 3- and 4-iodobenzoate, two reagents for iodination of proteins. *Appl Radiat Isot.* 1998;49:955–959.
35. Orlova A, Höglund J, Lubberink M, et al. Comparative biodistribution of the radiohalogenated (Br, I and At) antibody A33: implication for *in vivo* dosimetry. *Cancer Biother Radiopharm.* 2002;17:385–396.
36. Wållberg H, Orlova A. Slow internalization of anti-HER2 synthetic Affibody monomer ^{111}In-DOTA-$Z_{HER2:342-pep2}$: implications for development of labeled tracers. *Cancer Biother Radiopharm.* 2008;23:435–442.
37. Froidevaux S, Heppeler A, Eberle AN, et al. Preclinical comparison in AR4-2J tumor-bearing mice of four radiolabeled 1,4,7,10-tetraazacyclododecane-1,4,7,10-tetraacetic acid-somatostatin analogs for tumor diagnosis and internal radiotherapy. *Endocrinology.* 2000;141:3304–3312.
38. Austin CD, De Maziere AM, Pisacane PI, et al. Endocytosis and sorting of ErbB2 and the site of action of cancer therapeutics trastuzumab and geldanamycin. *Mol Biol Cell.* 2004;15:5268–5282.
39. Verel I, Visser GW, Boerman OC, et al. Long-lived positron emitters zirconium-89 and iodine-124 for scouting of therapeutic radioimmunoconjugates with PET. *Cancer Biother Radiopharm.* 2003;18:655–661.
40. Orlova A, Tolmachev V, Pehrson R, et al. Synthetic affibody molecules: a novel class of affinity ligands for molecular imaging of HER2-expressing malignant tumors. *Cancer Res.* 2007;67:2178–2186.
41. Tran T, Engfeldt T, Orlova A, et al. ^{99m}Tc-maEEE-$Z_{HER2:342}$, an Affibody molecule-based tracer for detection of HER2-expression in malignant tumors. *Bioconjug Chem.* 2007;18:1956–1964.